

Pressure Tuning of Electronic Correlations and Flat Bands in CsCr_3Sb_5

Maria Chatzileftheriou,^{1,2} Jonas B. Profe,¹ Ying Li,³ and Roser Valentí¹

¹*Institute for Theoretical Physics, Goethe University Frankfurt,
Max-von-Laue-Straße 1, 60438 Frankfurt a.M., Germany*

²*CPHT, CNRS, École polytechnique, Institut Polytechnique de Paris, 91120 Palaiseau, France*

³*MOE Key Laboratory for Nonequilibrium Synthesis and Modulation of Condensed Matter,
School of Physics, Xi'an Jiaotong University, Xi'an 710049, China*

CsCr_3Sb_5 is a newly identified strongly correlated kagome superconductor, characterized by non-Fermi-liquid behavior at elevated temperatures and intertwined charge- and spin-density-wave order below $T_{DW} \approx 54\text{K}$. Under external pressure, this order is suppressed and a superconducting phase emerges. This phase diagram, which closely resembles that of high- T_c superconductors, together with a kagome flat band near the Fermi level and possible antiferromagnetic order, has motivated extensive theoretical and experimental investigations. To better understand how pressure influences the ordered states, we present a systematic study of the evolution of the electronic properties under applied pressure. Performing DFT+DMFT (density functional theory combined with dynamical mean field theory) calculations, we uncover a complex interplay between the redistribution of spectral weight in the flat bands and the strength of electronic correlations under pressure. Our results further strengthen the interpretation that pressure effectively weakens electronic correlations through enhanced orbital hybridization. This, in turn, strongly suggests that superconductivity emerges as a direct consequence of the suppression of the system's ordered phase.

Flat-band systems have emerged as a major focus of research in recent years [1–5], driven by their unique potential to host both strong electronic correlations [6–9] due to the quenched kinetic energy within the flat band, and non-trivial topological effects [2, 10]. This combination provides an ideal platform for exploring how topology and interactions intertwine to produce novel quantum phenomena, including charge ordering and unconventional superconductivity [1, 11–18]. Kagome materials provide a natural platform for this physics, as their geometry produces Dirac points, van Hove singularities, flat bands, and nontrivial topology [19–26] in various combinations across different compounds [9, 27–31].

CsCr_3Sb_5 has recently been identified as a novel kagome material that, owing to its crystal structure and electron filling, features flat bands near the Fermi level and strong orbital-selective electronic correlations [32–34]. At ambient pressure, the system is a correlated bad metal, exhibiting simultaneous charge and spin density wave order below $\sim 54\text{K}$ [34–40]. Under the application of hydrostatic pressure, the two ordered phases separate in temperature [33]. With increasing pressure, these ordered states are eventually suppressed, and a superconducting dome emerges at higher pressures (between ~ 4 – 10 GPa) and low temperatures (below $\sim 6.4\text{ K}$) [41, 42]. At present, neither the nature of the spin and charge fluctuations nor the mechanism underlying the unconventional superconductivity is fully understood. This combination of a rich phase diagram and strong electronic correlations suggests that CsCr_3Sb_5 is the long-sought strongly coupled counterpart of the weakly coupled AV_3Sb_5 family of kagome metals [28, 43, 44].

To address these experimental questions, theoretical studies based on density functional theory (DFT) [45] have shown that the multi-orbital nature of the low-energy bands arises primarily from the Cr 3-*d* orbitals [33, 34, 46], which hybridize with the antimony p_z orbital. At the DFT level, un-

der ambient pressure the flat bands are found to be located between ~ 100 – 300 meV above the Fermi level, while the experimental findings suggest a much smaller distance from E_F [34]. This discrepancy is believed to originate from the insufficient treatment of correlation effects within DFT. The relevance of strong correlations is suggested by the bad metallic behavior observed in both Angle-Resolved Photoemission Spectroscopy (ARPES), low temperature specific heat data and resistivity measurements highlighting the need for an accurate treatment of electronic correlations [33, 35].

A few works have rigorously included the effect of strong electronic interactions in the system, using either the Slave-Spin [47–50] or the Dynamical Mean-Field Theory (DMFT) [51] approach [35, 52–54]. These studies, focusing on the system under ambient pressure, have revealed that correlations indeed shift the flat bands closer to E_F , through a large renormalization of certain orbitals. These studies further identify the Hund's exchange as a key factor of orbital-selective mass enhancement [35], placing the material within the framework of Hund's metal physics, where a decoupling between different orbital characters occurs [55, 56].

The influence of hydrostatic pressure on the electronic structure of CsCr_3Sb_5 has not yet been theoretically explored beyond the DFT framework. In particular, the pressure evolution of the flat bands and their potential connection to the suppression of magnetic and charge order, as well as to the emergence of superconductivity, remain open questions. In this work, we address these issues by investigating the multi-orbital nature of band renormalization and spectral-weight redistribution under ambient and finite pressures, incorporating many-body effects within a DFT+DMFT approach.

Methods — The structure optimization simulations under pressure were performed with the projector-augmented wave

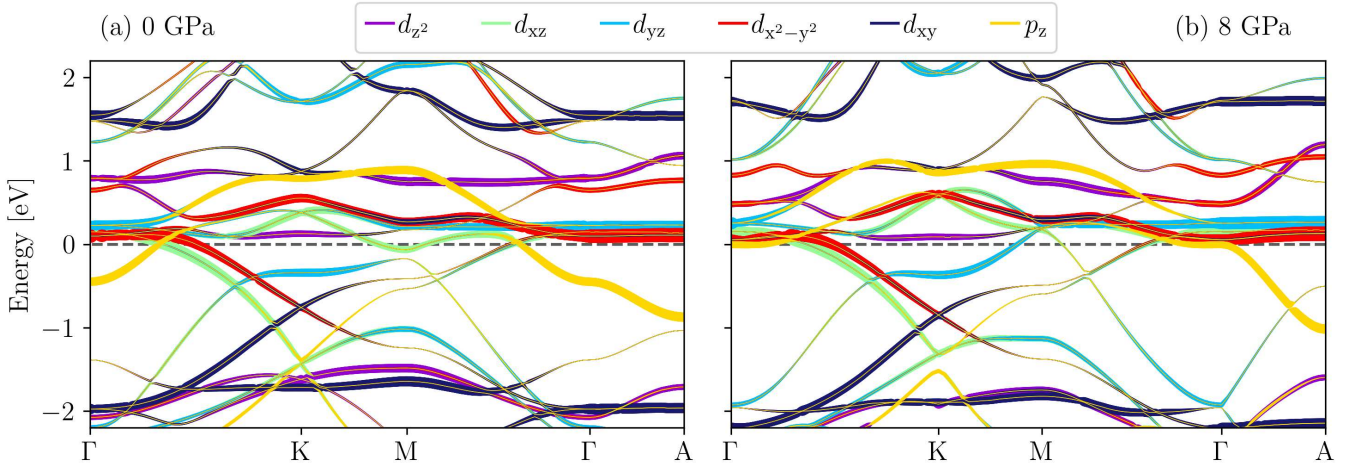


FIG. 1. The bandstructure of CsCr_3Sb_5 along the high-symmetry-path for 0 Gpa pressure in panel (a) and for 8 Gpa pressure in panel (b) from DFT. The orbital weights for a the indicated selectioion of orbitals are color-coded by their linewidth. The width of the dots corresponds to the weight of the respective orbital. We observe that pressure induces a reduction in size of the electron pocket near the Γ point with largest weight on the Antimony p_z orbital

method [57, 58] as implemented in the VASP code [59, 60]. We used the generalized gradient approximation (GGA) [61] as exchange-correlation functional and included magnetism. Relaxations were performed assuming a ferromagnetic order of the Cr atoms. Convergence of the properties of interest was achieved for a $6 \times 6 \times 6$ k-mesh and an energy cutoff of 520 eV. We find that the structural parameters of the experimental ambient-pressure structure [33](0 GPa) are closely reproduced by the theoretically relaxed structure at 1.19 GPa (see SM [62]), which serves as a reference for theory–experiment comparison. Similarly, the experimental structure at 4 GPa aligns well with the theoretical structure at 5.19 GPa, with the resulting lattice constants reported in SM [62]. Considering that the experimental X-ray data were obtained at finite temperature [33], while our simulations are performed at zero temperature with a specific choice of exchange-correlation functional and magnetic configuration, the level of agreement is remarkably good.

In order to estimate the hopping parameters for the structures under pressures, we have performed *ab initio* density functional theory calculations with the linearized augmented plane wave (LAPW) method [63]. The Perdew-Burke-Ernzerhof generalized gradient approximation [61] was used, with a mesh of 1000 k points in the first Brillouin zone and RK_{\max} was set to 7. The hopping parameters were obtained through the Wannier function projection formalism implemented in Wien2wannier [64] and Wannier90 [65]. The calculations were double-checked with the full potential local orbital (FPLO) code [66]. The valence electrons per unit cell are $34 = 1 \times 1(\text{Cs-}6s1) + 3 \times 6(\text{Cr-}3d5,4s1) + 5 \times 3(\text{Sb-}5p3)$. Our effective tight-binding model includes $31 = 1 \times 1(\text{Cs-s}) + 3 \times 5(\text{Cr-d}) + 5 \times 3(\text{Sb-p})$ orbitals with fixed filling of 34 electrons. As described in Ref. [52], the dominant orbitals around Fermi energy are Cr d_{xz} , d_{yz} , $d_{x^2-y^2}$ and Sb p_z . As visualized

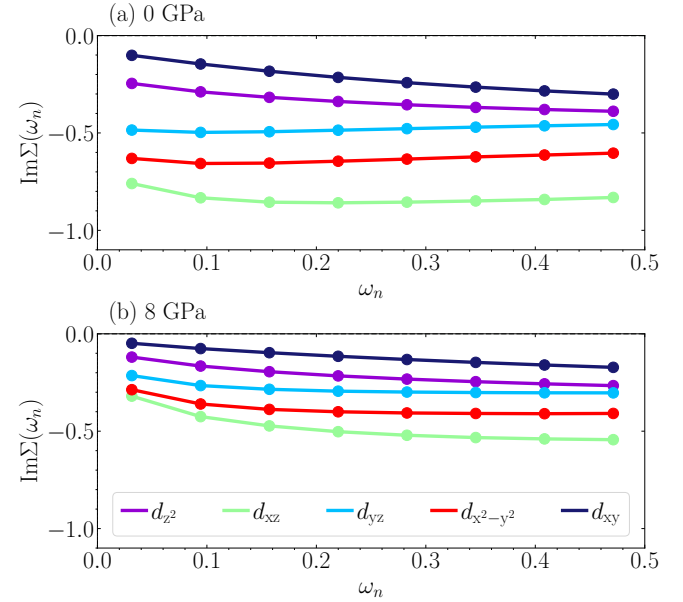


FIG. 2. Imaginary part of the orbital-resolved self-energy as a function of Matsubara frequencies for pressure $P = 0$ GPa in panel (a) and $P = 8$ GPa in panel (b). The self-energies are overall smaller for a finite pressure, revealing that the system is less correlated. At $P = 0$ GPa we find strong orbital selectivity, with the d_{xz} , d_{yz} and $d_{x^2-y^2}$ orbitals being strongly correlated.

in the SM [62], the dominant hoppings of all these orbitals increase under pressure due to the reduction in interatomic distances. The DFT bandstructures at ambient conditions and 8 GPa pressure are visualized in Fig.1 (a) and (b), respectively.

For the purpose of accounting for the effect of electronic correlations we employ state-of-the-art Dynamical Mean Field Theory (DMFT) [51]. Within DMFT, we treat the five

d -orbitals of the three Cr atoms as interacting and all the rest of the orbitals as non-interacting, using a continuous-time hybridization expansion Quantum Monte Carlo impurity solver *w2dynamics* [67, 68]. We fix the temperature to $T = 1/100 \text{ eV}^{-1} \simeq 116 \text{ K}$, for which the system is at its normal metallic state. To determine the interaction parameters within the Cr-3d manifold, we perform constrained RPA calculation [69, 70], see SM [62] for details. We obtain the average interaction parameters $U \sim 1.5\text{--}2.0 \text{ eV}$ and $J = 0.2\text{--}0.3U$ in line with previous cRPA calculations [71, 72] for other kagome compounds and $d - dp$ type interaction parameters. This choice of interaction parameters is consistent with the choice of correlated d -orbitals and p orbitals being projected out on the level of the Green's function [69, 73]. We, hence, set the Coulomb repulsion at $U = 2.0 \text{ eV}$ and the Hund's exchange coupling at $J = 0.6 \text{ eV}$ (in the SM [62] we include a discussion on the role of the J value). Due to the inclusion of both d and p orbitals, an unphysical double counting contribution appears, and the relevant term needs to be subtracted from the self-energy. To this end, we employ the *fully localized limit (fl)* double counting scheme, which assumes the correlations included in the non-interacting problem to represent the atomic limit of the lattice problem [68, 74].

Results — In order to analyze the strength of correlations in the system, we plot in Fig. 2 the imaginary part of the self-energy as a function of Matsubara frequencies, for the different Cr d -orbitals. The $P = 0 \text{ GPa}$ results are shown in panel (a) and the $P = 8 \text{ GPa}$ ones in panel (b). At ambient pressure the system is correlated and strongly orbital selective, with the d_{xz} , d_{yz} and $d_{x^2-y^2}$ orbitals exhibiting significantly larger mass enhancement and bad metallic behavior compared to the d_z and d_{xy} , in agreement with previous studies [52, 53]. The effect of finite pressure (Fig. 2(b)) is to decrease the overall degree of correlations in the material, with all the self-energies becoming smaller and more metallic. In fact, for the less correlated orbitals d_z and d_{xy} , $\text{Im}\Sigma \rightarrow 0$ in the limit $\omega_n \rightarrow 0$, while for the more correlated orbitals d_{xz} , d_{yz} and $d_{x^2-y^2}$ in the same limit, $\text{Im}\Sigma$ obtains a much smaller absolute value, compared to the situation at $P = 0 \text{ GPa}$. Moreover, the previously observed strong orbital differentiation gets suppressed correspondingly but does not vanish entirely.

We now examine how changes in the correlation strength between the two cases are manifested in the spectral properties of the system. In Fig. 3 the momentum-resolved spectral functions corresponding to $P = 0 \text{ GPa}$ (Fig. 3 (a)) and $P = 8 \text{ GPa}$ (Fig. 3 (b)) are plotted along the high-symmetry path $\Gamma\text{-K}\text{-M}\text{-}\Gamma\text{-A}$ as a function of energy, accompanied by the local density of states (DOS) in Fig. 3 (c)). At ambient pressure ($P = 0 \text{ GPa}$) the large correlations lead to a flat band, which is located almost at (but still slightly above) E_F , in contrast to its $\sim 100\text{--}150 \text{ meV}$ distance from E_F in DFT. A second flat band with reduced weight is found slightly below E_F , in agreement to various ARPES measurements [34–36]. In fact, the literature includes contradicting experimental and theoretical evidence, depending on the sensitivity of each method, suggesting a flat band above or below E_F . In this work, we

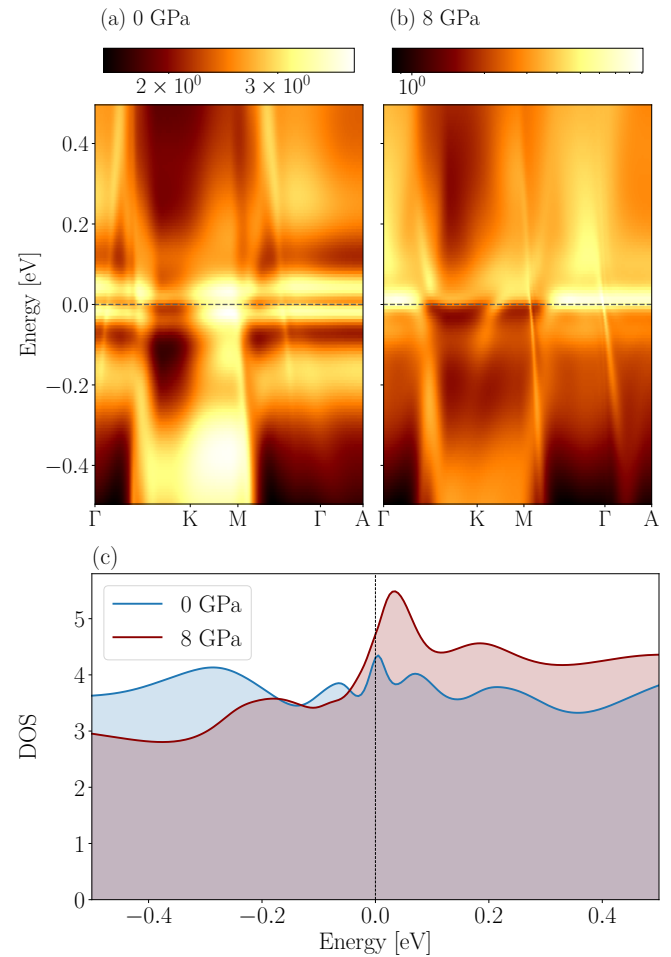


FIG. 3. DFT+DMFT spectral function (in color) as a function of momentum and energy (panel (a) $P = 0 \text{ GPa}$, panel (b) $P = 8 \text{ GPa}$), accompanied by the local density of states (DOS) (panel (c)). The spectral function plots reveal that the flat bands are located very close to the Fermi energy ($E_F = 0$). At $P = 8 \text{ GPa}$, weight is redistributed within the flat band, which remains highly weighted only at parts of the momentum path. The DOS at $P = 0 \text{ GPa}$ is more strongly renormalized compared to $P = 8 \text{ GPa}$, as a direct consequence of the larger degree of correlations, observed from the self-energy.

resolve the possibility of two flat bands appearing in the spectral function, above and below E_F respectively, as observed in experiments[34–36]. The application of $P = 8 \text{ GPa}$ hydrostatic pressure induces a large redistribution of weight, due to the reduction of the correlations. The system appears to be more coherent, with a high density of states within the positive energy flat band, only at parts of the Brillouin Zone.

The DFT+DMFT orbitally-resolved DOS, see Fig. 4, reveals that the main contribution to the flat bands around E_F comes from the d_{xz} , d_{yz} and $d_{x^2-y^2}$ orbitals, which are the most strongly correlated ones, as discussed above. Importantly, the peaks corresponding to those orbitals are a few meV away from E_F , for both values of pressure $P = 0 \text{ GPa}$, (Fig. 4 (a)) and $P = 8 \text{ GPa}$ (Fig. 4 (b)), indicating a pinning behavior near the Fermi-level. Focusing on the density of states away from

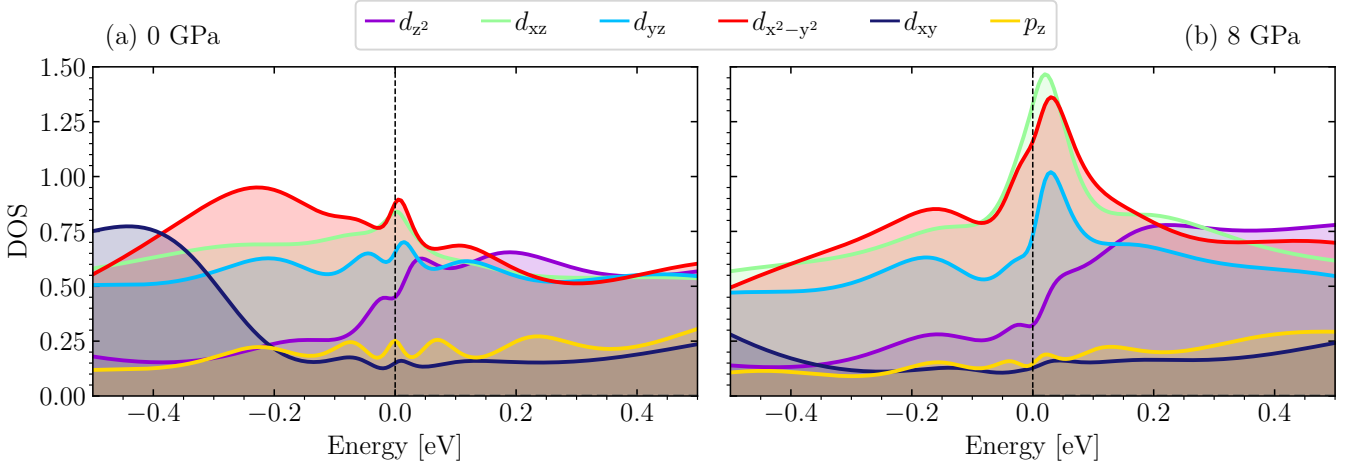


FIG. 4. DFT+DMFT orbitally-resolved density of states (DOS) at $P = 0$ GPa in panel (a) and $P = 8$ GPa in panel (b). The three orbitals that mainly contribute to the flat bands are d_{xz} , d_{yz} and $d_{x^2-y^2}$, which are the most strongly correlated orbitals, as illustrated by the self-energy data.

E_F , one immediately confirms that at zero pressure the system is more correlated, as the high-energy features have more spectral weight, while the low energy quasiparticle peaks get strongly renormalized. Further, we find that the Cr- d_{z^2} and the Sb- p_z still contribute a large density-of states in the energy-range in which the flat bands were located in DFT. This is important as scanning tunneling spectroscopy (STS) measurements are mainly sensitive to these orbitals. Therefore, the observed orbital selectivity potentially explains the discrepancy of the strong correlations suggested by the bad metallic behavior in ARPES [33, 35] and a recent STS measurement observing no strong energy shifts of a flat-band compared to DFT [40].

Discussions — In the SM [62] the electronic occupancies of the two cases ($P = 0$ GPa and $P = 8$ GPa) are discussed. The main observation is that both in DFT and in DMFT all orbitals are in proximity to - but not at - half-filling. The mass enhancement of a correlated metal is often controlled by the orbital occupancies [75]. In the regime of strong interactions, if one or more orbitals approach half-filling, even an orbital-selective Mott transition can take place [76–78]. In that case, the electronic states with those orbital characters become strongly renormalized and localize, behaving effectively as insulating, while the other orbitals remain itinerant and metallic. We observe that the d_{xz} orbital is the one that in DMFT approaches its individual half-filling, by departing from its DFT value. This result is in perfect agreement with the observation that the d_{xz} orbital has the largest self-energy and is the most strongly renormalized one.

However, we observe that the difference between the occupancies calculated for $P = 0$ GPa and $P = 8$ GPa is negligible. Thus, this variation cannot explain the large, qualitatively different behavior of the self-energy for d_{xz} , d_{yz} and $d_{x^2-y^2}$, among the two values of pressure. The culprit behind this qualitatively different behavior can be identified as the spectral weight redistribution within the flat bands and its inter-

play with the increased kinetic energy due to pressure. Therefore, if we want to link the low-temperature ordered phases observed in CsCr_3Sb_5 to the electronic correlations in the normal state, we must focus on the spectral composition of the flat bands.

At ambient condition, we observe in DFT+DMFT a large, essentially non-dispersive weight at the Fermi-level, indicating a large degree of localization of the electronic degrees of freedom. This agrees with the observation of magnetism in DFT, with a large magnetic moment of $1.7\mu_B$. As mentioned above, under pressure, the DFT+DMFT DOS at the Fermi-level is enhanced, while the flat band becomes more dispersive. This points towards a transition from localized incoherent (zero-dimensional) electronic degrees of freedom to an effectively 2-dimensional (albeit still rather incoherent) electronic system. This change is reflected on the DFT level by a reduction of the magnetic moment to $1.46\mu_B$ at $P = 8$ GPa.

While we cannot reach the Fermi-liquid regime in our DMFT analysis, these results in combination with prior DFT calculations and experiments reveal a few key aspects for the ordered states [33]. First of all, the clear signature of a structural instability in phonon calculations [46] indicates that the density wave order is at least partially driven by the phonon sector. When entering a charge-density-wave phase, the Cr kagome lattice is slightly distorted resulting in reduced geometric frustration, thus magnetic order is less penalized and can form. This strong intertwining of magnetism and charge ordering implies that both sectors will be relevant in understanding the superconducting order, as in e.g. the alkali doped fullerenes [79]. Our results on the other hand indicate, that pressure reduces correlations and changes the effective dimensionality of the electronic dispersion. Thus, under pressure the material evolves from a regime dominated by localized flat-band physics to one where more dispersive states appear at the Fermi level and become entangled with the flat bands. Overall, this suggests that while flat bands may play a pivotal

role in the magnetic state, they are not the primary ingredient for superconductivity. Fully disentangling this interplay will require future studies that approach the ordered phases from a strongly correlated perspective, complemented by alternative routes to tuning correlations—such as the chemical substitution strategy recently explored by Crispino *et al.* [54].

Conclusion — We systematically investigated the role of pressure as a tuning parameter in controlling the electronic properties and ordered states of CsCr_3Sb_5 . Through DFT+DMFT calculations, we reveal a clear interplay between flat-band spectral weight redistribution and electronic correlations under pressure. Our results show that pressure consistently weakens correlations and orbital selectivity through enhanced hybridization and kinetic contributions, leading to reduced magnetic moments – as suggested by DFT results – and the possible suppression of long-range order. These findings strongly support the view that superconductivity emerges from the destabilization of the ordered phase. Together, our work helps reconcile differing experimental results, clarifies the transition from localized to two-dimensional behavior under pressure, and explains key trends in the phase diagram. Moreover, when combined with recent studies [33, 46], our results suggest a delicate and important interplay between electronic and phononic degrees of freedom.

We would like to thank Fang Xie, Qimiao Si, Matteo Crispino and Giorgio Sangiovanni for useful discussions at the various stages of the work. M. C., J. P. and R. V. acknowledge support by the Deutsche Forschungsgemeinschaft (DFG, German Research Foundation) for funding through projects QUAST-FOR5249 (449872909) (projects P4). The authors gratefully acknowledge the computing time provided to them at the NHR Center NHR@SW at Goethe-University Frankfurt (project number p0026387). This is funded by the Federal Ministry of Education and Research, and the state governments participating on the basis of the resolutions of the GWK for national high performance computing at universities (www.nhr-verein.de/unsere-partner).

spective for magnetism and superconductivity,” *Contemporary Physics* **66**, 1–38 (2025).

- [6] Haoyu Hu, Gautam Rai, Lorenzo Crippa, Jonah Herzog-Arbeitman, Dumitru Călugăru, Tim Wehling, Giorgio Sangiovanni, Roser Valentí, Alexei M Tsvelik, and B Andrei Bernevig, “Symmetric Kondo lattice states in doped strained twisted bilayer graphene,” *Physical review letters* **131**, 166501 (2023).
- [7] Anushree Datta, Maria Jose Calderon, Alberto Camjayi, and Elena Bascones, “Heavy quasiparticles and cascades without symmetry breaking in twisted bilayer graphene,” *Nature Communications* **14**, 5036 (2023).
- [8] Gautam Rai, Lorenzo Crippa, Dumitru Călugăru, Haoyu Hu, Francesca Paoletti, Luca de’ Medici, Antoine Georges, B. Andrei Bernevig, Roser Valentí, Giorgio Sangiovanni, and Tim Wehling, “Dynamical Correlations and Order in Magic-Angle Twisted Bilayer Graphene,” *Phys. Rev. X* **14**, 031045 (2024).
- [9] Hanoh Lee, Churhli Lyi, Taehee Lee, Hyeonhui Na, Jinyoung Kim, Sangjae Lee, Younsik Kim, Anil Rajapitamahuni, Asish K. Kundu, Elio Vescovo, Byeong-Gyu Park, Changyoung Kim, Charles H. Ahn, Frederick J. Walker, Ji Seop Oh, Bo Gyu Jang, Youngkuk Kim, Byungmin Sohn, and Tuson Park, “Co-existing Kagome and Heavy Fermion Flat Bands in YbCr_6Ge_6 ,” (2025), [arXiv:2509.04902 \[cond-mat.str-el\]](https://arxiv.org/abs/2509.04902).
- [10] Sebastiano Peotta and Päivi Törmä, “Superfluidity in topologically nontrivial flat bands,” *Nature Communications* **6** (2015), 10.1038/ncomms9944.
- [11] Yu-Ping Lin, Chunxiao Liu, and Joel E. Moore, “Complex magnetic and spatial symmetry breaking from correlations in kagome flat bands,” *Phys. Rev. B* **110**, L041121 (2024).
- [12] Dumitru Călugăru, Aaron Chew, Luis Elcoro, Yuanfeng Xu, Nicolas Regnault, Zhi-Da Song, and B Andrei Bernevig, “General construction and topological classification of crystalline flat bands,” *Nature Physics* **18**, 185–189 (2022).
- [13] Mingu Kang, Shiang Fang, Linda Ye, Hoi Chun Po, Jonathan Denlinger, Chris Jozwiak, Aaron Bostwick, Eli Rotenberg, Efthimios Kaxiras, Joseph G Checkelsky, *et al.*, “Topological flat bands in frustrated kagome lattice CoSn,” *Nature communications* **11**, 4004 (2020).
- [14] Charles Mielke III, Debarchan Das, J-X Yin, H Liu, R Gupta, Y-X Jiang, Marisa Medarde, X Wu, Hechang C Lei, J Chang, *et al.*, “Time-reversal symmetry-breaking charge order in a kagome superconductor,” *Nature* **602**, 245–250 (2022).
- [15] Wei Zhang, Xinyou Liu, Lingfei Wang, Chun Wai Tsang, Zheyu Wang, Siu Tung Lam, Wenyan Wang, Jianyu Xie, Xuefeng Zhou, Yusheng Zhao, Shanmin Wang, Jeff Tallon, Kwing To Lai, and Swee K. Goh, “Nodeless Superconductivity in Kagome Metal CsV3Sb_5 with and without Time Reversal Symmetry Breaking,” *Nano Letters* **23**, 872–879 (2023), pMID: 36662599.
- [16] Jia-Xin Yin, Yu-Xiao Jiang, Xiaokun Teng, Md. Shafayat Hosain, Sougata Mardanya, Tay-Rong Chang, Zijin Ye, Gang Xu, M. Michael Denner, Titus Neupert, Benjamin Lienhard, Han-Bin Deng, Chandan Setty, Qimiao Si, Guoqing Chang, Zurab Guguchia, Bin Gao, Nana Shumiya, Qi Zhang, Tyler A. Cochran, Daniel Multer, Ming Yi, Pengcheng Dai, and M. Zahid Hasan, “Discovery of Charge Order and Corresponding Edge State in Kagome Magnet FeGe ,” *Phys. Rev. Lett.* **129**, 166401 (2022).
- [17] Elliott Rosenberg, Jonathan M. DeStefano, Yucheng Guo, Ji Seop Oh, Makoto Hashimoto, Donghui Lu, Robert J. Birgeneau, Yongbin Lee, Liqin Ke, Ming Yi, and Jiun-Haw Chu, “Uniaxial ferromagnetism in the kagome metal TbV_6Sn_6 ,” *Phys. Rev. B* **106**, 115139 (2022).

- [1] Yuan Cao, Valla Fatemi, Shiang Fang, Kenji Watanabe, Takashi Taniguchi, Efthimios Kaxiras, and Pablo Jarillo-Herrero, “Unconventional superconductivity in magic-angle graphene superlattices,” *Nature* **556**, 43–50 (2018).
- [2] Päivi Törmä, Sebastiano Peotta, and Bogdan A Bernevig, “Superconductivity, superfluidity and quantum geometry in twisted multilayer systems,” *Nature Reviews Physics* **4**, 528–542 (2022).
- [3] Joseph G. Checkelsky, B. Andrei Bernevig, Piers Coleman, Qimiao Si, and Silke Paschen, “Flat bands, strange metals and the Kondo effect,” *Nature Reviews Materials* **9**, 509–526 (2024).
- [4] Valentin Crépel, Nicolas Regnault, and Raquel Queiroz, “Chiral limit and origin of topological flat bands in twisted transition metal dichalcogenide homobilayers,” *Communications Physics* **7** (2024), 10.1038/s42005-024-01641-6.
- [5] Hideo Aoki, “Flat bands in condensed-matter systems – per-

[18] Lixuan Zheng, Zhimian Wu, Ye Yang, Linpeng Nie, Min Shan, Kuanglv Sun, Dianwu Song, Fanghang Yu, Jian Li, Dan Zhao, Shunjiao Li, Baolei Kang, Yanbing Zhou, Kai Liu, Ziji Xiang, Jianjun Ying, Zhenyu Wang, Tao Wu, and Xianhui Chen, “Emergent charge order in pressurized kagome superconductor CsV_3Sb_5 ,” *Nature* **611**, 682–687 (2022).

[19] II Mazin, Harald O Jeschke, Frank Lechermann, Hunpyo Lee, Mario Fink, Ronny Thomale, and Roser Valentí, “Theoretical prediction of a strongly correlated Dirac metal,” *Nature communications* **5**, 4261 (2014).

[20] Maximilian L. Kiesel and Ronny Thomale, “Sublattice interference in the kagome Hubbard model,” *Phys. Rev. B* **86**, 121105 (2012).

[21] Yong Hu, Samuel M.L. Teicher, Brenden R. Ortiz, Yang Luo, Shuting Peng, Linwei Huai, Junzhang Ma, Nicholas C. Plumb, Stephen D. Wilson, Junfeng He, and Ming Shi, “Topological surface states and flat bands in the kagome superconductor CsV_3Sb_5 ,” *Science Bulletin* **67**, 495–500 (2022).

[22] Yong Hu, Xianxin Wu, Brenden R. Ortiz, Sailong Ju, Xinlong Han, Junzhang Ma, Nicholas C. Plumb, Milan Radovic, Ronny Thomale, Stephen D. Wilson, Andreas P. Schnyder, and Ming Shi, “Rich nature of Van Hove singularities in Kagome superconductor CsV_3Sb_5 ,” *Nature Communications* **13**, 2220 (2022).

[23] Jia-Xin Yin, Biao Lian, and M Zahid Hasan, “Topological kagome magnets and superconductors,” *Nature* **612**, 647–657 (2022).

[24] Francesco Ferrari, Federico Becca, and Roser Valentí, “Charge density waves in kagome-lattice extended Hubbard models at the van Hove filling,” *Physical Review B* **106**, L081107 (2022).

[25] Mingu Kang, Sunje Kim, Yuting Qian, Paul M. Neves, Linda Ye, Junseo Jung, Denny Puntel, Federico Mazzola, Shiang Fang, Chris Jozwiak, Aaron Bostwick, Eli Rotenberg, Jun Fuji, Ivana Vobornik, Jae-Hoon Park, Joseph G. Checkelsky, Bohm-Jung Yang, and Riccardo Comin, “Measurements of the quantum geometric tensor in solids,” *Nature Physics* **21**, 110–117 (2024).

[26] Qi Wang, Hechang Lei, Yanpeng Qi, and Claudia Felser, “Intriguing kagome topological materials,” *npj Quantum Materials* **10** (2025), 10.1038/s41535-025-00790-3.

[27] Rui Lou, Liqin Zhou, Wenhua Song, Alexander Fedorov, Zhi-jun Tu, Bei Jiang, Qi Wang, Man Li, Zhonghao Liu, Xuezhi Chen, Oliver Rader, Bernd Büchner, Yujie Sun, Hongming Weng, Hechang Lei, and Shancai Wang, “Orbital-selective effect of spin reorientation on the Dirac fermions in a non-charge-ordered kagome ferromagnet Fe_3Ge ,” *Nature Communications* **15** (2024), 10.1038/s41467-024-53343-w.

[28] Brenden R. Ortiz, Paul M. Sarte, Eric M. Kenney, Michael J. Graf, Samuel M. L. Teicher, Ram Seshadri, and Stephen D. Wilson, “Superconductivity in the \mathbb{Z}_2 kagome metal KV_3Sb_5 ,” *Phys. Rev. Mater.* **5**, 034801 (2021).

[29] Qiangwei Yin, Zhijun Tu, Chunsheng Gong, Shangjie Tian, and Hechang Lei, “Structures and physical properties of v-based kagome metals CsV_6Sb_6 and $\text{CsV}_8\text{Sb}_{12}$,” *Chinese Physics Letters* **38**, 127401 (2021).

[30] He Zhao, Hong Li, Brenden R. Ortiz, Samuel M. L. Teicher, Takamori Park, Mengxing Ye, Ziqiang Wang, Leon Balents, Stephen D. Wilson, and Ilija Zeljkovic, “Cascade of correlated electron states in the kagome superconductor CsV_3Sb_5 ,” *Nature* **599**, 216–221 (2021).

[31] Chunyu Guo, Glenn Wagner, Carsten Putzke, Dong Chen, Kaize Wang, Ling Zhang, Martin Gutierrez-Amigo, Ion Errea, Maia G. Vergniory, Claudia Felser, Mark H. Fischer, Titus Neupert, and Philip J. W. Moll, “Correlated order at the tipping point in the kagome metal CsV_3Sb_5 ,” *Nature Physics* **20**, 579–584 (2024).

[32] Haoyu Hu and Qimiao Si, “Coupled topological flat and wide bands: Quasiparticle formation and destruction,” *Science Advances* **9** (2023), 10.1126/sciadv.adg0028.

[33] Yi Liu, Zi-Yi Liu, Jin-Ke Bao, Peng-Tao Yang, Liang-Wen Ji, Si-Qi Wu, Qin-Xin Shen, Jun Luo, Jie Yang, Ji-Yong Liu, *et al.*, “Superconductivity under pressure in a chromium-based kagome metal,” *Nature* **632**, 1032–1037 (2024).

[34] Zehao Wang, Yucheng Guo, Hsiao-Yu Huang, Fang Xie, Yuefei Huang, Bin Gao, Ji Seop Oh, Han Wu, Jun Okamoto, Ganessa Channagowdara, *et al.*, “Spin excitations and flat electronic bands in a Cr-based kagome superconductor,” *Nature Communications* **16**, 7573 (2025).

[35] Yidian Li, Yi Liu, Xian Du, Siqi Wu, Wenxuan Zhao, Kaiyi Zhai, Yinqi Hu, Senyao Zhang, Houke Chen, Jieyi Liu, *et al.*, “Electron correlation and incipient flat bands in the Kagome superconductor CsCr_3Sb_5 ,” *Nature Communications* **16**, 3229 (2025).

[36] Shuting Peng, Yulei Han, Yongkai Li, Jianchang Shen, Yu Miao, Yang Luo, Linwei Huai, Zhipeng Ou, Hongyu Li, Ziji Xiang, Zhengtai Liu, Dawei Shen, Makoto Hashimoto, Donghui Lu, Yugui Yao, Zhenhua Qiao, Zhiwei Wang, and Junfeng He, “Flat bands and distinct density wave orders in correlated Kagome superconductor CsCr_3Sb_5 ,” (2024), arXiv:2406.17769 [cond-mat.supr-con].

[37] Shuto Suzuki, Takemi Kato, Yongkai Li, Kosuke Nakayama, Zhiwei Wang, Seigo Souma, Kenichi Ozawa, Miho Kitamura, Koji Horiba, Hiroshi Kumigashira, Takashi Takahashi, Yugui Yao, and Takafumi Sato, “Evolution of band structure in the kagome superconductor $\text{Cs}(\text{V}_{1-x}\text{Cr}_x)_3\text{Sb}_5$: Toward universal understanding of charge density wave and superconducting phase diagrams,” *Phys. Rev. B* **110**, 165104 (2024).

[38] Zihao Huang, Chenchao Xu, Yande Que, Yi Liu, Ranjith Shivarajao, Zheng Jue Tong, Amit Kumar, Chao Cao, Guang-Han Cao, Hong-Jun Gao, and Bent Weber, “Controlling an alternating magnetic spin density wave in the kagome magnet CsCr_3Sb_5 ,” (2025), arXiv:2510.05018 [cond-mat.str-el].

[39] Siyu Cheng, Keyu Zeng, Yi Liu, Christopher Candelier, Ziqiang Wang, Guang-Han Cao, and Ilija Zeljkovic, “Frieze charge-stripes in a correlated kagome superconductor CsCr_3Sb_5 ,” (2025), arXiv:2510.06168 [cond-mat.str-el].

[40] Yunxing Li, Peigen Li, Taimin Miao, Rui Xu, Yongqing Cai, Neng Cai, Bo Liang, Han Gao, Hanbo Xiao, Yongzhen Jiang, Jiefeng Cao, Fangyuan Zhu, Hongkun Wang, Jincheng Xie, Jingcheng Li, Zhongkai Liu, Chaoyu Chen, Yunwei Zhang, X. J. Zhou, Dingyong Zhong, Huichao Wang, Jianwei Huang, and Donghui Guo, “Exotic Surface Stripe Orders in Correlated Kagome Metal CsCr_3Sb_5 ,” (2025), arXiv:2510.12888 [cond-mat.str-el].

[41] Wang, Qi and Lei, Hechang and Qi, Yanpeng and Felser, Claudia, “Intriguing kagome topological materials,” *npj Quantum Materials* **10**, 72 (2025).

[42] Siqi Wu, Chenchao Xu, Xiaoqun Wang, Hai-Qing Lin, Chao Cao, and Guang-Han Cao, “Flat-band enhanced antiferromagnetic fluctuations and superconductivity in pressurized CsCr_3Sb_5 ,” *Nature Communications* **16**, 1375 (2025).

[43] Eric M Kenney, Brenden R Ortiz, Chennan Wang, Stephen D Wilson, and Michael J Graf, “Absence of local moments in the kagome metal KV_3Sb_5 as determined by muon spin spectroscopy,” *Journal of Physics: Condensed Matter* **33**, 235801 (2021).

[44] Brenden R. Ortiz, Lídia C. Gomes, Jennifer R. Morey, Michal Winiarski, Mitchell Bordelon, John S. Mangum, Iain W. H. Oswald, Jose A. Rodriguez-Rivera, James R. Neilson,

Stephen D. Wilson, Elif Ertekin, Tyrel M. McQueen, and Eric S. Toberer, “New kagome prototype materials: discovery of KV_3Sb_5 , RbV_3Sb_5 , and CsV_3Sb_5 ,” *Phys. Rev. Mater.* **3**, 094407 (2019).

[45] W. Kohn and L. J. Sham, “Self-Consistent Equations Including Exchange and Correlation Effects,” *Phys. Rev.* **140**, A1133–A1138 (1965).

[46] Chenchao Xu, Siqi Wu, Guo-Xiang Zhi, Guanghan Cao, Jian-hui Dai, Chao Cao, Xiaoqun Wang, and Hai-Qing Lin, “Altermagnetic ground state in distorted Kagome metal $CsCr_3Sb_5$,” *Nature Communications* **16**, 3114 (2025).

[47] L. de’Medici, A. Georges, and S. Biermann, “Orbital-selective Mott transition in multiband systems: Slave-spin representation and dynamical mean-field theory,” *Phys. Rev. B* **72**, 205124 (2005).

[48] Rong Yu and Qimiao Si, “Mott transition in multiorbital models for iron pnictides,” *Phys. Rev. B* **84**, 235115 (2011).

[49] Rong Yu and Qimiao Si, “ $U(1)$ slave-spin theory and its application to Mott transition in a multiorbital model for iron pnictides,” *Phys. Rev. B* **86**, 085104 (2012).

[50] Matteo Crispino, Maria Chatzileftheriou, Tommaso Gorni, and Luca de’ Medici, “Slave-spin mean field for broken-symmetry states: Néel antiferromagnetism and its phase separation in multiorbital Hubbard models,” *Phys. Rev. B* **107**, 155149 (2023).

[51] Antoine Georges, Gabriel Kotliar, Werner Krauth, and Marcelo J. Rozenberg, “Dynamical mean-field theory of strongly correlated fermion systems and the limit of infinite dimensions,” *Rev. Mod. Phys.* **68**, 13–125 (1996).

[52] Fang Xie, Yuan Fang, Ying Li, Yuefei Huang, Lei Chen, Chandan Setty, Shouvik Sur, Boris Yakobson, Roser Valentí, and Qimiao Si, “Electron correlations in the kagome flat band metal $CsCr_3Sb_5$,” *Phys. Rev. Res.* **7**, L022061 (2025).

[53] Yilin Wang, “Heavy fermions in frustrated Hund’s metal with portions of incipient flat bands,” *Phys. Rev. B* **111**, 035127 (2025).

[54] Matteo Crispino, Niklas Witt, Stefan Enzner, Tommaso Gorni, Luca de’ Medici, Domenico Di Sante, and Giorgio Sangiovanni, “Tunable Electronic Correlations in 135-Kagome Metals,” (2025), arXiv:2512.22576 [cond-mat.str-el].

[55] Kristjan Haule and Gabriel Kotliar, “Coherence-incoherence crossover in the normal state of iron oxypnictides and importance of Hund’s rule coupling,” *New journal of physics* **11**, 025021 (2009).

[56] Antoine Georges, Luca de’ Medici, and Jernej Mravlje, “Strong correlations from Hund’s coupling,” *Annu. Rev. Condens. Matter Phys.* **4**, 137–178 (2013).

[57] Blöchl, P. E., “Projector augmented-wave method,” *Phys. Rev. B* **50**, 17953–17979 (1994).

[58] G. Kresse and D. Joubert, “From ultrasoft pseudopotentials to the projector augmented-wave method,” *Phys. Rev. B* **59**, 1758–1775 (1999).

[59] G. Kresse and J. Furthmüller, “Efficiency of ab-initio total energy calculations for metals and semiconductors using a plane-wave basis set,” *Comput. Mater. Sci.* **6**, 15–50 (1996).

[60] J. Hafner, “*Ab-initio* simulations of materials using vasp: Density-functional theory and beyond,” *J. Comput. Chem.* **29**, 2044 (2008).

[61] John P. Perdew, Kieron Burke, and Matthias Ernzerhof, “Generalized Gradient Approximation Made Simple,” *Phys. Rev. Lett.* **77**, 3865–3868 (1996).

[62] See Supplemental Material for details of the DFT and cRPA calculations, an analysis of the orbital occupancies and of the effect of Hund’s exchange coupling on the system. The Supplemental Material also contains Refs. [80, 81].

[63] Peter Blaha, Karlheinz Schwarz, Fabien Tran, Robert Laskowski, Georg K. H. Madsen, and Laurence D. Marks, “WIEN2k: An APW+lo program for calculating the properties of solids,” *The Journal of Chemical Physics* **152**, 074101 (2020).

[64] Jan Kuneš, Ryotaro Arita, Philipp Wissgott, Alessandro Toschi, Hiroaki Ikeda, and Karsten Held, “Wien2wannier: From linearized augmented plane waves to maximally localized Wannier functions,” *Computer Physics Communications* **181**, 1888–1895 (2010).

[65] Giovanni Pizzi, Valerio Vitale, Ryotaro Arita, Stefan Blügel, Frank Freimuth, Guillaume Géranton, Marco Gibertini, Dominik Gresch, Charles Johnson, Takashi Koretsune, Julen Ibañez-Azpiroz, Hyungjun Lee, Jae-Mo Lihm, Daniel Marchand, Antimo Marrazzo, Yuriy Mokrousov, Jamal I Mustafa, Yoshiro Nohara, Yusuke Nomura, Lorenzo Paulatto, Samuel Poncé, Thomas Ponweiser, Junfeng Qiao, Florian Thöle, Stepan S Tsirkin, Małgorzata Wierzbowska, Nicola Marzari, David Vanderbilt, Ivo Souza, Arash A Mostofi, and Jonathan R Yates, “Wannier90 as a community code: new features and applications,” *Journal of Physics: Condensed Matter* **32**, 165902 (2020).

[66] Klaus Koepernik and Helmut Eschrig, “Full-potential nonorthogonal local-orbital minimum-basis band-structure scheme,” *Phys. Rev. B* **59**, 1743 (1999).

[67] Emanuel Gull, Andrew J. Millis, Alexander I. Lichtenstein, Alexey N. Rubtsov, Matthias Troyer, and Philipp Werner, “Continuous-time Monte Carlo methods for quantum impurity models,” *Reviews of Modern Physics* **83**, 349–404 (2011).

[68] Markus Wallerberger, Andreas Hausoel, Patrik Gunacker, Alexander Kowalski, Nicolaus Parragh, Florian Goth, Karsten Held, and Giorgio Sangiovanni, “w2dynamics: Local one- and two-particle quantities from dynamical mean field theory,” *Comput. Phys. Commun.* **235**, 388–399 (2019).

[69] F. Aryasetiawan, M. Imada, A. Georges, G. Kotliar, S. Biermann, and A. I. Lichtenstein, “Frequency-dependent local interactions and low-energy effective models from electronic structure calculations,” *Phys. Rev. B* **70**, 195104 (2004).

[70] Merzuk Kaltak, “Merging GW with DMFT,” (2015), 10.25365/THESIS.3809.

[71] Domenico Di Sante, Bongjae Kim, Werner Hanke, Tim Wehling, Cesare Franchini, Ronny Thomale, and Giorgio Sangiovanni, “Electronic correlations and universal long-range scaling in kagome metals,” *Phys. Rev. Res.* **5**, L012008 (2023).

[72] Feihu Liu, Changxu Liu, Maolin Zeng, and Qiyi Zhao, “Electron correlations in kagome metals AV_3Sb_5 ($A = K, Rb, Cs$)”, (2025), arXiv:2506.09864 [cond-mat.str-el].

[73] Jonas B. Profe, Jakša Vučičević, P. Peter Stavropoulos, Malte Rösner, Roser Valentí, and Lennart Klebl, “Exact downfolding and its perturbative approximation,” (2025), arXiv:2507.16916 [cond-mat.str-el].

[74] Czyžyk, M. T. and Sawatzky, G. A., “Local-density functional and on-site correlations: The electronic structure of La_2CuO_4 and $LaCuO_3$,” *Phys. Rev. B* **49**, 14211–14228 (1994).

[75] Antoine Georges, Luca de’ Medici, and Jernej Mravlje, “Strong Correlations from Hund’s Coupling,” *Annual Review of Condensed Matter Physics* **4**, 137–178 (2013).

[76] V.I. Anisimov, I.A. Nekrasov, D.E. Kondakov, T.M. Rice, and M. Sigrist, “Orbital-selective Mott-insulator transition in $Ca_{2-x}Sr_xRuO_4$,” *The European Physical Journal B* **25**, 191–201 (2002).

[77] Akihisa Koga, Norio Kawakami, T. M. Rice, and Manfred Sigrist, “Orbital-Selective Mott Transitions in the Degenerate

Hubbard Model,” *Phys. Rev. Lett.* **92**, 216402 (2004).

[78] Luca de’ Medici, S. R. Hassan, Massimo Capone, and Xi Dai, “Orbital-Selective Mott Transition out of Band Degeneracy Lifting,” *Phys. Rev. Lett.* **102**, 126401 (2009).

[79] Yusuke Nomura, Shiro Sakai, Massimo Capone, and Ryotaro Arita, “Unified understanding of superconductivity and Mott transition in alkali-doped fullerides from first principles,” *Science Advances* **1** (2015), 10.1126/sciadv.1500568.

[80] de’Medici, Luca, “14 Hund’s Metals Explained,” *The Physics of Correlated Insulators, Metals, and Superconductors* .

[81] Chatzileftheriou, Maria and Kowalski, Alexander and Berović, Maja and Amaricci, Adriano and Capone, Massimo and De Leo, Lorenzo and Sangiovanni, Giorgio and de’ Medici, Luca, “Mott Quantum Critical Points at Finite Doping,” *Phys. Rev. Lett.* **130**, 066401 (2023).

Supplemental Material

Pressure Tuning of Electronic Correlations and Flat Bands in CsCr_3Sb_5

Maria Chatzieleftheriou,^{1,2} Jonas B. Profe,¹ Ying Li,³ and Roser Valentí¹

¹*Institute for Theoretical Physics, Goethe University Frankfurt,*

Max-von-Laue-Straße 1, 60438 Frankfurt a.M., Germany

²*CPHT, CNRS, École polytechnique, Institut Polytechnique de Paris, 91120 Palaiseau, France*

³*MOE Key Laboratory for Nonequilibrium Synthesis and Modulation of Condensed Matter, School of Physics, Xi'an Jiaotong University, Xi'an 710049, China*

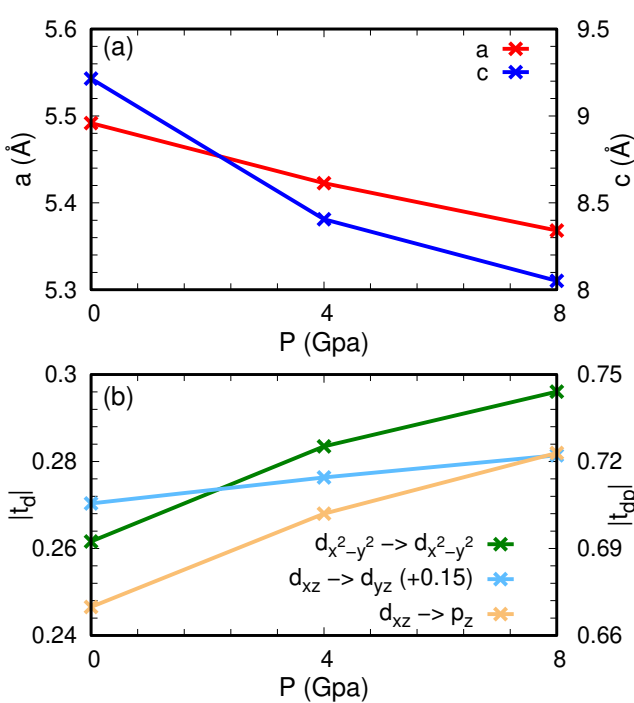


FIG. 1. Pressure dependence of the (a) lattice constants a (left axis) and c (right axis) as well as (b) dominant hopping parameters within Cr-Cr ($|t_d|$, left axis) and Cr-Sb ($|t_{dp}|$, right axis).

DETAILS OF THE DFT CALCULATIONS

In Fig. 1(a) we visualize the dependence of the lattice parameters on pressure. From these calculations we observe that the structural data of the experimental structure [1] at ambient pressure (0 GPa) are rather well reproduced by the theoretically relaxed structure at 1.19 GPa, therefore defining the effective zero of pressure for our theoretical simulations. The careful relaxation of the structure appears to be crucial for an accurate comparison between theory and experiment. As described in Ref. [2], the dominant orbitals around Fermi energy are Cr d_{xz} , d_{yz} , and $d_{x^2-y^2}$, Sb p_z . We therefore plot in Fig. 1(b) the dominant hopping parameters within these orbitals. All of

	d_{xy}	d_{xz}	d_{yz}	d_{z^2}	$d_{x^2-y^2}$
d_{xy}	2.01	1.41	1.39	1.17	1.18
d_{xz}	0.33	2.31	1.26	1.22	1.17
d_{yz}	0.31	0.51	2.24	1.16	1.21
d_{z^2}	0.54	0.47	0.45	2.42	1.87
$d_{x^2-y^2}$	0.55	0.46	0.47	0.29	2.47

TABLE I. Interaction parameters for the ambient pressure case as extracted from cRPA. We give the Density-density elements of the coulomb tensor in the upper triangular parts and Hund's coupling values J in the lower triangular part in blue.

them increase under pressure due to the reduction in interatomic distances, as expected.

CONSTRAINED RANDOM PHASE APPROXIMATION

We performed the cRPA calculations with VASP. To this end, we first performed a self-consistent calculation for the relaxed structures on a denser k -mesh of $12 \times 12 \times 9$ and an energy cutoff of 600 eV, with a gaussian broadening of 0.05 eV. Next, we wannierized the 31 orbital model as described in the main text and performed a projector cRPA with the 15 Cr-d orbitals chosen as the correlated space. To avoid k -point convergence issues from the renormalization of the projectors, we did not consider the long wavelength limit in our calculations [3]. We checked that the hierarchy of the values is not altered by the inclusion of the long-wavelength limit and that the broadening is not altering the screening as well. The cRPA interaction parameters for the ambient pressure case are shown in I.

ORBITAL OCCUPANCIES

In Table II the occupancies of the two cases ($P = 0$ GPa and $P = 8$ GPa) are listed extracted both from LDA and DMFT. Here, we observe that in DFT all orbitals are in proximity to - but not at - half-filling, which does not change drastically when treating correlations within DMFT. Therefore, the systems are in the regime in which Coulomb repulsion is not the

m	$n_m^{LDA}(0 \text{ GPa})$	$n_m(0 \text{ GPa})$	$n_m^{LDA}(8 \text{ GPa})$	$n_m(8 \text{ GPa})$
d_{z2}	0.485	0.477	0.485	0.479
d_{xz}	0.553	0.515	0.557	0.520
d_{yz}	0.390	0.437	0.401	0.439
$d_{x^2-y^2}$	0.405	0.459	0.412	0.453
d_{xy}	0.608	0.575	0.608	0.584
tot	4.882	4.927	4.926	4.951

TABLE II. Orbital occupancies for $P = 0 \text{ GPa}$ and $P = 8 \text{ GPa}$, obtained by DFT (second and fourth column) and DFT+DMFT (third and fifth column). The value of pressure does not affect significantly the individual orbital occupancies, which remain in proximity to half-filling.

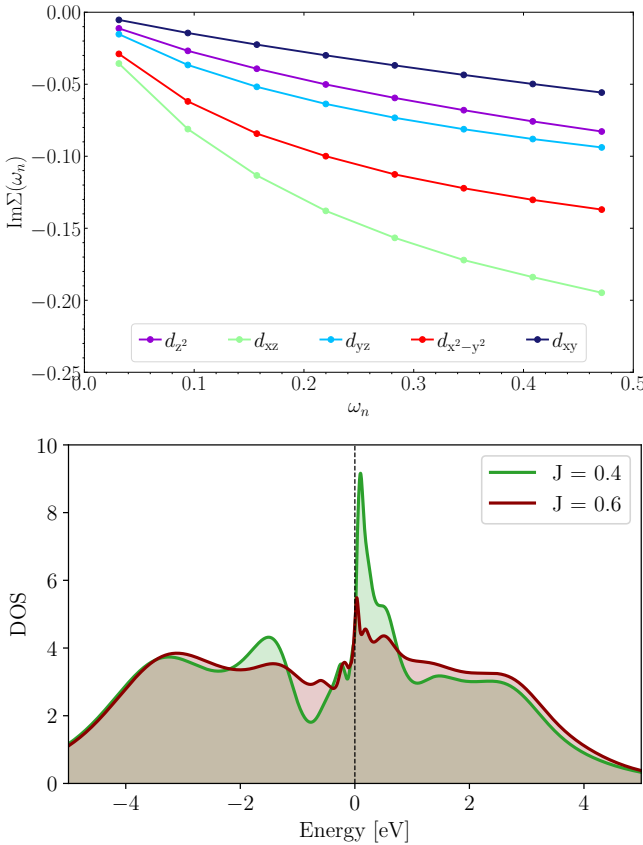


FIG. 2. Results of the system under $P = 8 \text{ GPa}$ pressure, with a Hund's coupling $J = 0.4 \text{ eV}$. **Upper panel:** Imaginary part of the self-energy per correlated orbital. The correlation strength is suppressed compared to $J = 0.6 \text{ eV}$, discussed in the main text. **Lower panel:** Total DOS of the system with $J = 0.4 \text{ eV}$, compared to the one with $J = 0.6 \text{ eV}$. The smaller self-energy gives rise to a larger peak around the Fermi energy without a general change in the form of the DOS.

only dominant interaction term, and Hund's physics becomes important [4, 5]. We observe that the most strongly corre-

lated d_{xz} orbital (it has the largest self-energy as discussed in the main text) is the one that in DMFT approaches its individual half-filling, by departing from its LDA value, both for $P = 0 \text{ GPa}$ and $P = 8 \text{ GPa}$. Overall, the difference in the orbital occupancies between the two pressure values are very small.

DEPENDENCE ON HUND'S EXCHANGE COUPLING

As discussed in the main text, by performing cRPA calculations we obtain the average interaction parameters $U \sim 1.5 - 2.0 \text{ eV}$ and $J = 0.2 - 0.3U$. Throughout this work, we have chosen to focus on the values $U = 2.0 \text{ eV}$ and $J = 0.3U = 0.6 \text{ eV}$. In Fig. we plot results for a smaller value of Hund's coupling $J = 0.2U = 0.4 \text{ eV}$, for the case of $P = 8 \text{ GPa}$. The imaginary part of the self-energy per correlated d -orbital is shown in the upper panel. We observe that the system is significantly less correlated compared to Fig.2 in the main text and, in particular, it is much less orbitally selective. These results are expected, since it is known that Hund's coupling is the term that favors orbital selectivity and enhances correlations. All orbitals exhibit a good Fermi liquid behavior, without alteration in the order of the correlation degree among the orbitals. In the lower panel of Fig. the total density of states is plotted by comparing the $J = 0.6 \text{ eV}$ and $J = 0.4 \text{ eV}$ cases. We reduction of correlations for $J = 0.4 \text{ eV}$ is reflected in the larger coherent peak around the Fermi level. However, it is interesting to notice that the overall behavior does not change drastically, with the main peak remaining above Fermi, still with distinctive features compared to the $P = 0 \text{ GPa}$ case.

[1] Yi Liu, Zi-Yi Liu, Jin-Ke Bao, Peng-Tao Yang, Liang-Wen Ji, Si-Qi Wu, Qin-Xin Shen, Jun Luo, Jie Yang, Ji-Yong Liu, *et al.*, “Superconductivity under pressure in a chromium-based kagome metal,” *Nature* **632**, 1032–1037 (2024).

[2] Fang Xie, Yuan Fang, Ying Li, Yuefei Huang, Lei Chen, Chandan Setty, Shouvik Sur, Boris Yakobson, Roser Valentí, and Qimiao Si, “Electron correlations in the kagome flat band metal CsCr_3Sb_5 ,” *Phys. Rev. Res.* **7**, L022061 (2025).

[3] Merzuk Kaltak, “Merging GW with DMFT,” [10.25365/THESIS.38099](https://arxiv.org/abs/10.25365/THESIS.38099).

[4] de' Medici, Luca, “14 Hund's Metals Explained,” *The Physics of Correlated Insulators, Metals, and Superconductors*.

[5] Chatzileftheriou, Maria and Kowalski, Alexander and Berović, Maja and Amaricci, Adriano and Capone, Massimo and De Leo, Lorenzo and Sangiovanni, Giorgio and de' Medici, Luca, “Mott Quantum Critical Points at Finite Doping,” *Phys. Rev. Lett.* **130**, 066401 (2023).